

Transport Theoretical Approach to the Nucleon Spectral Function in Nuclear Matter*

J. Lehr, M. Effenberger, H. Lenske, S. Leupold and U. Mosel
Institut für Theoretische Physik, Universität Giessen,
Heinrich-Buff-Ring 16, D-35392 Giessen, Germany
UGI-00-3

November 9, 2018

Abstract

The nucleon spectral function in infinite nuclear matter is calculated in a quantum transport theoretical approach. Exploiting the known relation between collision rates and correlation functions the spectral function is derived self-consistently. By re-inserting the spectral functions into the collision integrals the description of hard processes from the high-momentum components of wave functions and interactions is improved iteratively until convergence is achieved. The momentum and energy distributions and the nuclear matter occupation probabilities are in very good agreement with the results obtained from many-body theory.

PACS numbers: 21.65.+f, 24.10.Cn

Keywords: nuclear matter, many-body theory, nucleon spectral function

A longstanding problem of nuclear many-body theory is the question to what extent short-range correlations are contributing to the properties of nuclear matter. While the bulk properties of nuclear matter are mainly affected by long-range mean-field dynamics, the picture, however, changes if nuclei are probed at large energy and momentum transfer. The spectral functions,

*Work supported by BMBF, DFG and GSI Darmstadt

obtained for example from $A(e, e'p)X$ experiments [1], are in energy and momentum much wider spread than predicted by mean-field dynamics. Obviously, the high momentum and energy structure of spectral functions has important consequences for dynamical processes, e.g. sub-threshold particle production on nuclei.

An overall measure of short-range correlations in nuclear matter is the depletion of occupation probabilities in ground state momentum distributions by about 10%. The processes behind this number are such that states from inside the Fermi sphere are scattered into high momentum configurations which clearly are not of mean-field nature. As a result, a momentum distribution with a long high momentum tail is generated extending much beyond the Fermi surface. An important finding is that the magnitude and the shape of the high momentum component is almost independent of the system under consideration while the inner parts, especially in light nuclei, are affected by the shell structure and finite size effects. Hence, the high momentum tails of the spectral functions are likely to reflect a universal property of nuclear many-body dynamics at short distances.

Theoretically, many attempts have been made to understand short-range correlations in nuclei. Approaches based on nuclear many-body theory up to explanations referring to the QCD aspects of strong interactions [2] have been proposed. Obviously, before conclusions on non-standard phenomena can be drawn the many-body theoretical aspects of short-range correlations must be understood in detail. In fact, the results obtained from many-body theory are describing the available data rather satisfactorily. In recent years the theoretical results have converged, at least for the depletion of nuclear matter occupation probabilities. The majority of the model calculations are using Brueckner and Dirac-Brueckner techniques, see e.g. [3, 4, 5, 6, 7]. In [8] a correlation dynamical treatment was applied. Most of the approaches use the quasi-particle approximation, i.e. a sharp energy distribution for the nucleons is assumed (see e.g. [9]). Occupation probabilities in finite nuclei could be well described in a second RPA approach [10] and by polarization self-energies [11], respectively. The Dirac-Brueckner calculations in [7], including hole-hole propagation, led to an extended and numerically rather involved energy-momentum structure of self-energies. However, the net effect on binding energies and occupation probabilities was only moderate, but improving the agreement with empirical data.

Here, we investigate spectral functions in nuclear matter by quantum transport theory [12, 13], thereby taking up a proposal of Danielewicz and

Bertsch [14]. Indeed, the present study is motivated by our recent implementation of off-shell effects in a transport theoretical treatment of heavy-ion and other nuclear collisions [15, 16]. A sound theoretical basis how to treat off-shell effects in transport equations has been given in [17] (see also [18]). A central result of transport theory is that collision rates and correlation functions are directly related: The calculation of either of the two quantities requires the knowledge of the other one. Theoretically, this corresponds to a rather involved self-consistency problem for which a direct solution apparently does not exist. Similar to [7], a practical approach is obtained by an iterative procedure. Successive approximations for self-energies, spectral functions and collision integrals are obtained by re-inserting the corresponding quantities from previous cycles of the calculation until convergence is achieved. The method is discussed below. Results are presented and compared to the work of Benhar et al. [19] who calculated the nuclear matter spectral function within the framework of correlation-basis theory and of Ciofi degli Atti et al. [20, 21] who derived a global parameterization of spectral functions for finite nuclei and nuclear matter.

In quantum transport theory [12, 13] dynamical processes are described by the one-particle correlation functions

$$\begin{aligned} g^>(1, 1') &= -i\langle\Psi(1)\Psi^\dagger(1')\rangle \\ g^<(1, 1') &= i\langle\Psi^\dagger(1')\Psi(1)\rangle, \end{aligned} \tag{1}$$

where Ψ are the nucleon field operators in Heisenberg representation. They account for the non-stationary processes which introduce a coupling between causal and anti-causal single particle propagation. In other words, states from below and above the Fermi surface are dynamically mixed as discussed above. Correspondingly, in an interacting quantum system the single particle self-energy operator includes correlation self-energies $\Sigma^{<>}$ which couple particle and hole degrees of freedom [12, 13]. Obviously, $g^{<>}$ and $\Sigma^{<>}$ are closely related to each other and must be determined by those parts of the fundamental interactions producing non-stationary effects. The wanted relation is obtained from transport theory. After a Fourier transformation to energy-momentum representation one finds for the self energies [12]

$$\begin{aligned} \Sigma^>(\omega, p) &= g \int \frac{d^3p_2 d\omega_2}{(2\pi)^4} \frac{d^3p_3 d\omega_3}{(2\pi)^4} \frac{d^3p_4 d\omega_4}{(2\pi)^4} (2\pi)^4 \delta^4(p + p_2 - p_3 - p_4) \overline{|\mathcal{M}|^2} \\ &\times g^<(\omega_2, p_2) g^>(\omega_3, p_3) g^>(\omega_4, p_4) \end{aligned} \tag{2}$$

$$\begin{aligned} \Sigma^<(\omega, p) &= g \int \frac{d^3 p_2 d\omega_2}{(2\pi)^4} \frac{d^3 p_3 d\omega_3}{(2\pi)^4} \frac{d^3 p_4 d\omega_4}{(2\pi)^4} (2\pi)^4 \delta^4(p + p_2 - p_3 - p_4) \overline{|\mathcal{M}|^2} \\ &\times g^>(\omega_2, p_2) g^<(\omega_3, p_3) g^<(\omega_4, p_4), \end{aligned} \quad (3)$$

where $g = 4$ is the spin-isospin degeneracy factor and $\overline{|\mathcal{M}|^2}$ denotes the square of the nucleon-nucleon scattering amplitude, averaged over spin and isospin of the incoming nucleons and summed over spin and isospin of the outgoing nucleons. Since both $g^<>$ and $\Sigma^<>$ describe the correlation dynamics, the spectral function can be obtained from either of the two quantities as the difference over the cut along the energy real axis. In terms of the correlation propagators,

$$a(\omega, p) = i(g^>(\omega, p) - g^<(\omega, p)). \quad (4)$$

In a non-relativistic formulation the single particle spectral function is found explicitly as

$$a(\omega, p) = \frac{\Gamma(\omega, p)}{(\omega - \frac{p^2}{2m_N} - \text{Re}\Sigma(\omega, p))^2 + \frac{1}{4}\Gamma^2(\omega, p)}, \quad (5)$$

including the particle and hole nucleon self-energy Σ , which accounts for long-range mean-field dynamics. The width of the spectral distribution is determined by the imaginary part of the self-energy,

$$\Gamma(\omega, p) = 2\text{Im}\Sigma(\omega, p) = i(\Sigma^>(\omega, p) - \Sigma^<(\omega, p)). \quad (6)$$

From Eqs. (2), (3) it is apparent that the high momentum, i.e. short range, components of nuclear interactions are of primary importance for the energy-momentum spreading of the single particle strength. Obviously, the δ -shaped quasi-particle distribution is recovered for $\text{Im}\Sigma \rightarrow 0$, i.e. vanishing correlations.

The correlation propagators $g^<>$ are given by

$$g^<(\omega, p) = ia(\omega, p)f(\omega, p), \quad (7)$$

$$g^>(\omega, p) = -ia(\omega, p)(1 - f(\omega, p)) \quad (8)$$

in terms of the energy-momentum phase space distribution function $f(\omega, p)$. Since we are dealing with a system at $T = 0$, f reduces to

$$f(\omega, p) = \Theta(\omega_F - \omega) \quad (9)$$

with the Fermi energy ω_F . Therefore,

$$\Sigma^>(\omega, p) = 0, \quad \Gamma(\omega, p) = -i\Sigma^<(\omega, p) \quad \text{for } \omega \leq \omega_F \quad (10)$$

$$\Sigma^<(\omega, p) = 0, \quad \Gamma(\omega, p) = i\Sigma^>(\omega, p) \quad \text{for } \omega \geq \omega_F. \quad (11)$$

In order to obtain Γ , we have to calculate the self-energies $\Sigma^>$ and $\Sigma^<$. Since these quantities themselves depend on Γ via the spectral function $a(\omega, p)$, the calculation has to be done iteratively.

Diagrammatically, the particle- and hole-type transition rate $\Sigma^>$ and $\Sigma^<$, Eqs. (2) and (3), are of two-particle–one-hole (2p1h) and one-particle–two-hole (1p2h) structure, respectively. In this respect, they are of the same basic structure as the polarization self-energies considered in many-body theoretical descriptions. However, while in many-body theory the polarization self-energies are typically included perturbatively in lowest order only by performing the integrations over intermediate 2p1h and 1p2h states with quasi-particle spectral functions, e.g. in Ref. [19] and also Refs. [10, 11], we apply a more extended scheme accounting for higher order effects.

A first attempt to extend the many-body scheme to higher order calculations was made in [7]. Since, as expected, the computational effort was found to increase considerably approximations on spectral functions of particle intermediate states had to be invoked. An important aspect of the present transport theoretical approach is the fully self-consistent treatment of particle and hole strength function in each stage of the calculation. Within our iterative approach this is achieved by calculating the correlation self-energies with the self-consistently obtained spectral functions. Hence, the converged results include a non-perturbative summation of a whole series of np mh diagrams.

Dynamically, the strength of the transition rates is determined by the in-medium (off-shell) nucleon-nucleon scattering amplitude \mathcal{M} . We now make the extreme assumption of a constant transition amplitude, as is appropriate for the short-range part of the NN interaction. Neglecting the energy-momentum dependence of the amplitude clearly simplifies the computations. Then, \mathcal{M} contributes only as an overall multiplicative factor to the transition rates which, at a given density, may be treated as an empirical parameter

$\overline{\mathcal{M}}$. The self-energies $\Sigma^>$ and $\Sigma^<$ are then given by

$$\begin{aligned} \Sigma^>(\omega, p) = & -4i \frac{|\overline{\mathcal{M}}|^2}{(2\pi)^6} \int d\omega_3 \int d\omega_2 \int dp_3 p_3^2 \int dp_2 p_2^2 \frac{d \cos \vartheta_2}{p_{\text{tot}} p_3} a(\omega_2, p_2) \\ & \times f(\omega_2, p_2) a(\omega_3, p_3) (1 - f(\omega_3, p_3)) \int dp_4 p_4 a(\omega_4, p_4) (1 - f(\omega_4, p_4)) \end{aligned} \quad (12)$$

and

$$\begin{aligned} \Sigma^<(\omega, p) = & 4i \frac{|\overline{\mathcal{M}}|^2}{(2\pi)^6} \int d\omega_3 \int d\omega_2 \int dp_3 p_3^2 \int dp_2 p_2^2 \int \frac{d \cos \vartheta_2}{p_{\text{tot}} p_3} a(\omega_2, p_2) \\ & \times (1 - f(\omega_2, p_2)) a(\omega_3, p_3) f(\omega_3, p_3) \int dp_4 p_4 a(\omega_4, p_4) f(\omega_4, p_4) \end{aligned} \quad (13)$$

with $p_{\text{tot}} = |\vec{p} + \vec{p}_2|$, where four integrations due to the delta function and two over the azimuthal angles φ_2, φ_3 already have been carried out. The remaining six dimensional integrals were calculated on a (ω, p) -grid with boundaries $|\omega| \leq 0.5$ GeV and $p \leq p_{\text{max}} = 1.25$ GeV and a mesh size of 5 MeV in both directions.

In the present study we work in infinite nuclear matter at equilibrium with the Fermi momentum $p_F = 1.33 \text{ fm}^{-1}$, density $\rho = 0.16 \text{ fm}^{-3}$ and a binding energy per particle of $\omega_F = -16$ MeV. The real part of the self-energy $\text{Re}\Sigma$ is chosen to be independent of momentum and energy. In fact, a constant $\text{Re}\Sigma$ only serves to define the scale for the excitation energy ω which in our case is given by $\omega \geq \omega_F$. The energy and momentum dependent pieces of $\text{Re}\Sigma$ play a more important role because they will modify the pole structure of the propagators. Inside the Fermi sphere typically a quadratic momentum dependence is found leading to a scaling of the kinetic energy by an effective mass and a global compression of spectra will be found. Hence, leaving out the momentum dependence will affect the final results only to a minor degree. Neglecting the energy dependence might introduce larger uncertainties because this amounts to a violation of analyticity as expressed by the dispersion relation between real and imaginary parts of polarization self-energies. Since we do obtain an energy dependent imaginary part analyticity could in principle be restored by calculating $\text{Re}\Sigma$ dispersively. However, using a constant, energy independent transition matrix element clearly fails

for large positive energies because the imaginary part would continue to increase beyond any limit with the level density of two-particle states. Thus, the imaginary part of the self-energy is not available over the full range of energies necessary for solving the dispersion equation. Rather than introducing an energy cut-off as an additional free model parameter we decide at the present stage to completely neglect the energy dependence of $\text{Re}\Sigma$.

The average amplitude was adjusted such that the spectral functions obtained with many-body theoretical methods by Benhar et al. [19] are reproduced leading to $(|\overline{\mathcal{M}}|^2)^{1/2} = 207 \text{ MeV fm}^3$. Relating this value to on-shell processes would correspond to a constant cross section of about 20 mb. In Fig. 1 the full energy-momentum structure of the resulting nucleon spectral function

$$P(\omega, p) = N a(\omega, p) \quad (14)$$

is displayed, where N is a normalization constant. The same normalization as in the work of Benhar et al. [19] is used. Our results are in remarkable agreement with the calculations of Ciofi degli Atti et al. [21] as seen by comparing to Fig. 10 in that reference.

For a more quantitative comparison cuts for several momenta are shown in Fig. 2 as a function of energy ω below the Fermi surface and compared to the results of Ref. [19]. The agreement is surprisingly good considering the seemingly drastic approximation invoked for \mathcal{M} and the neglect of analyticity.

We conclude from this agreement that the spectral function of nuclear matter in the hole-sector is rather insensitive to the specific energy and momentum structure of the interaction once a fully self-consistent calculation is performed. The effect of self-consistency is illustrated in Fig. 2 where spectral functions obtained after the first iteration are compared to the fully converged results. The iteration scheme was initialized by choosing spectral functions with a constant width of 0.1 MeV as start value. On a level of about 30% global features, as e.g. the location and height of the peak structures, are described already by the first iteration. At first sight, this seems to support the perturbative approach usually applied in many-body theoretical approaches. However, during the self-consistency cycle strength is re-distributed from the peak into the tail regions. Hence, higher order polarization effects act in a similar way as increasing the effective coupling strength. The results show that the full transport theoretical calculation apparently leads to a self-consistent adjustment of spectral functions which

ultimately is dominated by phase space effects.

The agreement with the many-body calculations of [19] extends also to the single nucleon momentum distribution in nuclear matter defined as

$$n(p) = \int_{-\infty}^{\omega_F} d\omega P(\omega, p). \quad (15)$$

Results are displayed in Fig. 3. Again the agreement is close to perfect except for the increase of the distribution towards p_F , which is in contrast to the calculations of [19]. Calculations in a schematic model using an empirical form for $\Gamma(\omega, p)$ with parameters given in Ref. [23] show that this behaviour is a direct consequence of the missing analyticity in the self-energies. The schematic approach also confirms that the momentum dependence of $\text{Re}\Sigma$ indeed leads to minor effects in the bulk behaviour of the spectral functions except close to the Fermi surface. The momentum distribution is affected mainly in the extreme momentum tail where a steeper slope is found. In this context it is important to note that $n(p)$ must decrease stronger than $\mathcal{O}(\frac{1}{p^4})$ in order to have a convergent result for the kinetic energy distribution of the correlated ground state. The transport theoretical results in Fig. 3 fulfill this constraint.

Finally, we remark that the shape of the momentum distribution is closely related to the value of $\overline{\mathcal{M}}$: Increasing the value - corresponding to a stronger interaction amongst the nucleons - would increase the occupation of states above p_F and soften the Fermi edge, leading to a better description of the data in Fig. 3 for $p > p_F$.

Summarizing, correlations in nuclear matter have been described by an approach that allows to go beyond the perturbative level to which conventional many-body methods are constrained in practice. In a first application, the transition rates were calculated with a momentum independent nucleon-nucleon scattering amplitude. That a transport theoretical description with a simple approximation for the scattering amplitude could reproduce the momentum distribution obtained in state-of-the-art many-body calculations had already been observed by the authors of [14]. The results here show in addition that also the spectral functions are dominated by phase space effects rather than by the off-shell momentum structure of interactions. The excellent agreement of the nucleon spectral function at far-off-shell energies and momenta with those obtained in sophisticated state-of-the-art nuclear many-body calculations also provides some a-posteriori justification for the

method to include off-shell effects in nuclear transport calculations developed in Ref. [15].

Acknowledgements:

We are grateful to S. Fantoni for providing us with his spectral functions and to C. Ciofi degli Atti for helpful comments.

References

- [1] for a review see, e.g., P.K.A. de Witt Huberts, J. Phys. G (Nucl. Part. Phys.) **16** (1990) 507.
- [2] L. Frankfurt and M.I. Strikman, Phys. Rep. **76** (1981) 215.
- [3] A. Ramos, A. Polls and W.H. Dickhoff, Nucl. Phys. **A503** (1990) 1; A. Ramos, A. Polls and W.H. Dickhoff, Phys. Rev. **C43** (1991) 2239.
- [4] S. Fantoni and V.R. Pandharipande, Nucl. Phys. **A427** (1984) 473.
- [5] H. Mütter, G. Knehr and A. Polls, Phys. Rev. **C52** (1995) 2955.
- [6] F. de Jong and H. Lenske, Phys. Rev. **C54** (1996) 1488.
- [7] F. de Jong and H. Lenske, Phys. Rev. **C56** (1997) 154.
- [8] A. Peter, W. Cassing and J.M. Haeuser, Nucl. Phys. **A573** (1994) 93.
- [9] F. de Jong and R. Malfliet, Phys. Rev. **C44** (1991) 998.
- [10] F.J. Eckle, H. Lenske, G. Eckle, G. Graw, R. Hertenberger, H. Kader, F. Merz, H. Nann, P. Schiemenz and H.H. Wolter, Phys. Rev. **C39** (1989) 1662; F.J. Eckle, H. Lenske, G. Eckle, G. Graw, R. Hertenberger, H. Kader, H.J. Maier, F. Merz, H. Nann, P. Schiemenz and H.H. Wolter, Nucl. Phys. **A506** (1990) 159.
- [11] H. Lenske and J. Wambach, Phys. Lett. **B249** (1990) 377.
- [12] L.P. Kadanoff and G. Baym, Quantum Statistical Mechanics (Benjamin, New York, 1962).

- [13] W. Botermans and R. Malfliet, Phys. Rep. **198** (1990) 115.
- [14] G. Bertsch and P. Danielewicz, Phys. Lett. **B367** (1996) 55.
- [15] M. Effenberger and U. Mosel, Phys. Rev. **C60** (1999) 051901.
- [16] M. Effenberger, E.L. Bratkovskaya and U. Mosel, Phys. Rev. **C60** (1999) 044614.
- [17] S. Leupold, nucl-th/9909080; Nucl. Phys. **A**, in print.
- [18] W. Cassing and S. Juchem, Nucl. Phys. **A665** (2000) 385; nucl-th/9910052, Nucl. Phys. **A**, in print.
- [19] O. Benhar, A. Fabrocini and S. Fantoni, Nucl. Phys. **A505** (1989) 267; O. Benhar, A. Fabrocini and S. Fantoni, Nucl. Phys. **A550** (1992) 201.
- [20] C. Ciofi degli Atti, S. Simula, L.L. Frankfurt and M.I. Strickmann, Phys. Rev. **C44** R7 (1991).
- [21] C. Ciofi degli Atti and S. Simula, Phys. Rev. **C53** 1689 (1996).
- [22] S. Fantoni, private communication.
- [23] C. Mahaux and H. Ngo, Nucl. Phys. **A378** (1981) 285.
- [24] C. Ciofi degli Atti, E. Pace and G. Salme, Phys. Rev. **C43** (1991) 1153.

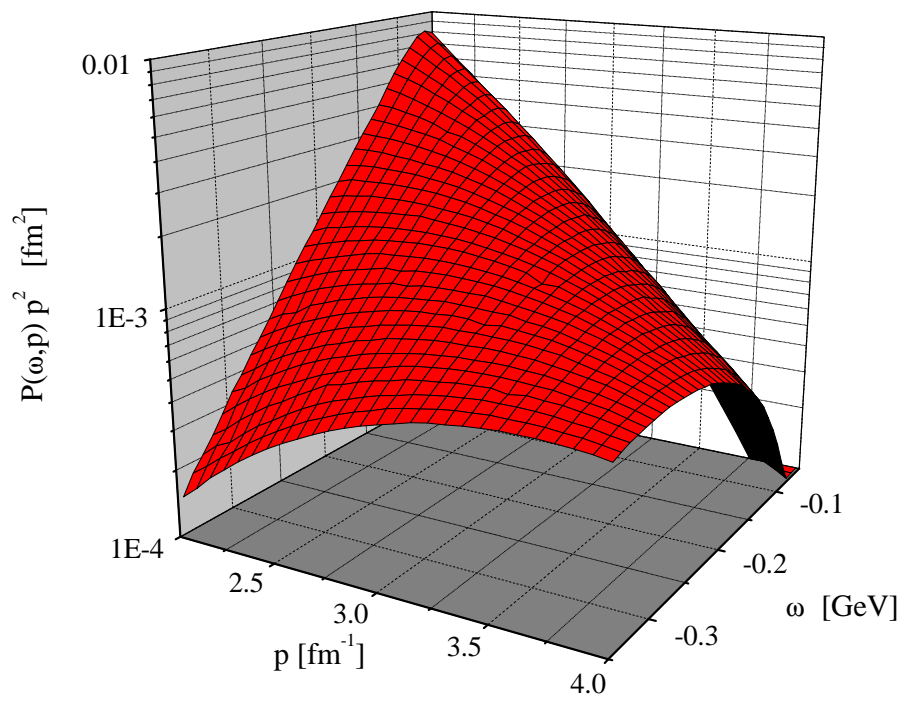


Figure 1: Energy and momentum dependence of the nucleon spectral function for energies below ω_F .

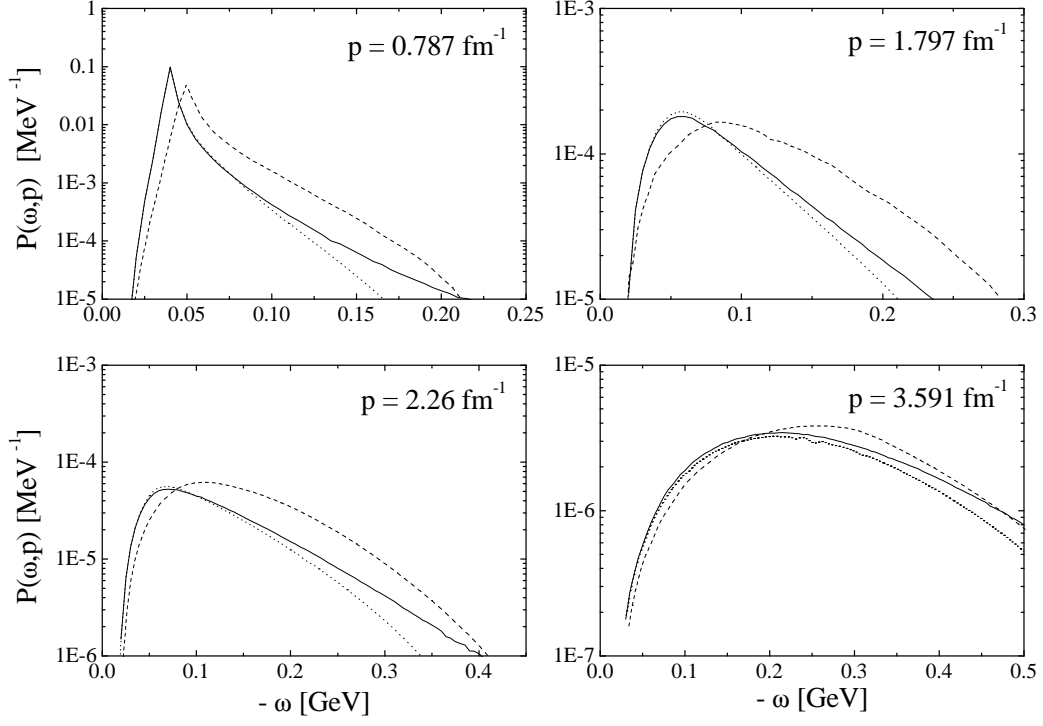


Figure 2: Nucleon spectral function for different constant momenta for energies below ω_F . The dotted curves have been obtained after the first iteration step using a constant initial width of 0.1 MeV (see text). The dashed curves show the results of Benhar et al. [19, 22].

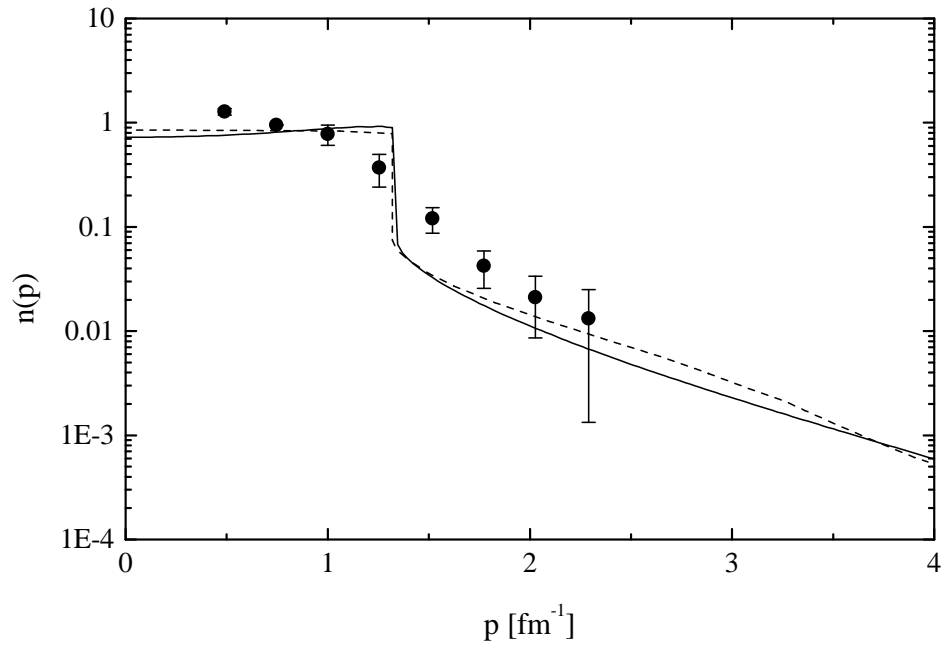


Figure 3: Momentum distribution in nuclear matter calculated from the spectral function. The dashed curve is the result from Benhar et al. [19]. The data are from [24].